Figure 4.8 : Y. Ohura's method of predicting generator angle

The predicted angle for time Th in the future is derived from the eight pieces of data indicated in Figure 4.8. These are the angles at time Tk before the present time t along with four values (Xm, Xm-1, Xm-2, Xm-3) at t-Tk, t-Th, t-2Th, t-3Th, respectively. and the angles at the current time t and in addition three values for this time minus increments of Th (Xn, Xn-1, Xn-2, Xn-3). The curve is estimated through equations (4.7) to (4.11).

$$X^* = Xn + \lambda\, d_n + \mu\, d_{n\text{-}1} \qquad (4.7)$$

where,

$$d_n = Xn\text{-}Xn\text{-}1 \;,\; d_{n\text{-}1} = Xn\text{-}1\text{-}Xn\text{-}2 \;,\; d_{n\text{-}2} = Xn\text{-}2\text{-}Xn\text{-}3 \qquad (4.8)$$

$$d_m = Xm\text{-}Xm\text{-}1 \;,\; d_{m\text{-}1} = Xm\text{-}1\text{-}Xm\text{-}2 \;,\; d_{m\text{-}2} = Xm\text{-}2\text{-}Xm\text{-}3 \qquad (4.9)$$

$$\lambda = (d_n d_{m\text{-}2} - d_m d_{n\text{-}2}) / (d_{n\text{-}1} d_{m\text{-}2} - d_{m\text{-}1} d_{n\text{-}2}) \qquad (4.10)$$

$$\mu = (d_{n\text{-}1} d_m - d_{m\text{-}1} d_n) / (d_{n\text{-}1} d_{m\text{-}2} - d_{m\text{-}1} d_{n\text{-}2}) \qquad (4.11)$$

Values of 40 ms and 20 ms were selected for Th and Tk, respectively, in order to predict accurately and to provide an acceptable operating time. Those values also match approximately with the 150 ms moving window used in the previous models. A simulation of the present prediction algorithm calculation is shown in Figure 4.9. It also presents a comparison with the second order auto-regressive model. The simulation case is the same as for Figure 4.7.
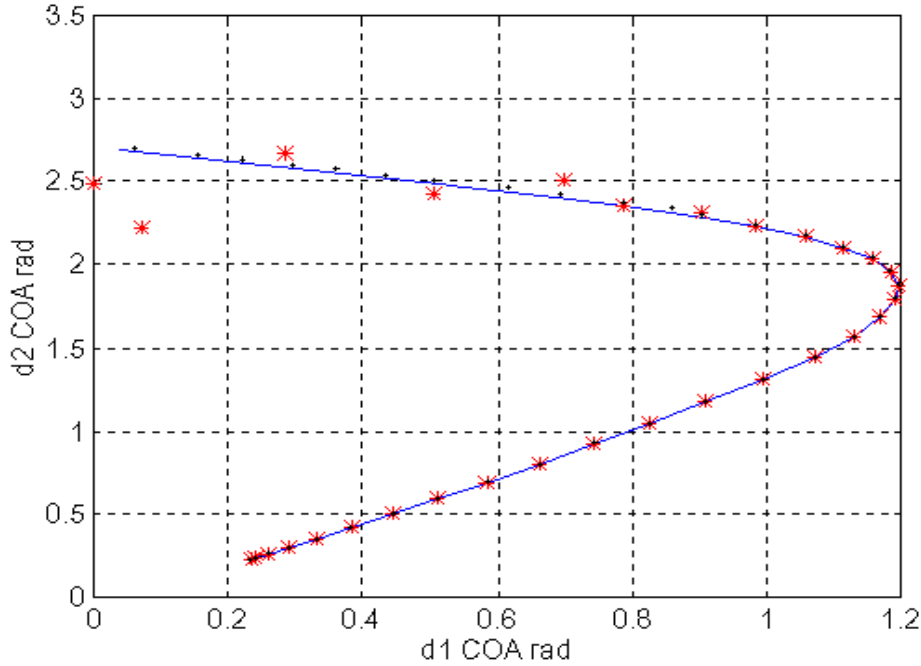
(* : Y. Ohura model & +: auto-regressive model & full: real trajectory)
Figure 4.9: Comparison between Y.Ohura and 2nd -order Auto-Regressive Models

Using the equation (4.7), only one value is predicted at 40 ms ahead of time. This prediction is then used in the calculation of the next value. After about 7 iterative steps of applying (4.7), the prediction diverges from the real trajectory. That is, to say that with a generator angle measurement sampling rate of 20 ms, the prediction could only be conducted over a period of 140 ms whereas 160 ms data window is required to set up the different parameters of the model. As for the former models, the post-fault path is predicted until it reaches a potential energy peak or until the time of the prediction passes over the 140 ms threshold value.

4.3 Stability boundary detection

The crossing point of the predicted post-fault trajectory and the potential energy boundary surface is obtained by setting the directional derivative of the potential energy along the trajectory equal to zero. However, due to the complexity of the stability region, the predicted post-fault trajectory may not cross the stability boundary and stay in the stability region whereas the directional derivative was set to zero. Then, to get closer to the p.e.b.s., the maximum of potential energy along a ray starting at the last point of the prediction and the post-fault s.e.p. is calculated. In the event where no maximum is encountered, the Ball-Drop method is used to find out whether the trajectory has already crossed the p.e.b.s.

The directional derivative is the dot product of the gradient and a unit vector parallel to the speed vector. Therefore, it requires the calculation of the gradient of the potential energy. Neglecting the damping, the swing equation of the ith machine is given by

$$M_i \frac{d\tilde{w}_i}{dt} = P_i - P_{ei}(\underline{\tilde{d}}) - \frac{M_i}{M_t} Pcoa(\underline{\tilde{d}}) \qquad i=1,...,n \qquad (4.12)$$

The right-hand sides of (4.12) represent the accelerating powers. They can be put in a vector form yielding

$$\underline{f}(\underline{\tilde{d}}) = \begin{bmatrix} P_1 - P_{e1}(\underline{\tilde{d}}) - \dfrac{M_1}{M_t} Pcoa(\underline{\tilde{d}}) \\ P_2 - P_{e2}(\underline{\tilde{d}}) - \dfrac{M_2}{M_t} Pcoa(\underline{\tilde{d}}) \\ \vdots \\ P_n - P_{en}(\underline{\tilde{d}}) - \dfrac{M_n}{M_t} Pcoa(\underline{\tilde{d}}) \end{bmatrix} \qquad (4.13)$$

The negative of the vector of accelerating powers is the potential energy gradient. It is given by

$$\nabla \underline{V}_{pe} = -\left[\underline{f}(\underline{\tilde{d}}) \right]^T \qquad (4.14)$$

The normalized speed vector on the trajectory is

$$\Rightarrow \underline{u} = \begin{bmatrix} \tilde{w}_1 \\ \tilde{w}_2 \\ \vdots \\ \tilde{w}_n \end{bmatrix} \frac{1}{\sqrt{\tilde{w}_1^2 + \tilde{w}_2^2 + ... + \tilde{w}_n^2}} \qquad (4.15)$$

The dot product of (33) and (34) is the directional derivative expressed as

$$\nabla \underline{V}_{pe} \cdot \underline{u} = -\sum_{i=1}^{n} \frac{f_i(\underline{\tilde{d}}) * (\tilde{w}_i)}{\sqrt{\tilde{w}_1^2 + ... + \tilde{w}_n^2}} \qquad (4.16)$$

As mentioned before, the crossing point is obtained by setting this directional derivative equal to zero. Therefore, it is the point which coordinates satisfy

$$\sum_{i=1}^{n} f_i(\underline{\tilde{d}}) . \tilde{w}_i = 0$$

$$\sum_{i=1}^{n} \left[P_i - P_{ei}(\underline{\tilde{d}}) - \frac{M_i}{M_t} Pcoa(\underline{\tilde{d}}) \right] . \tilde{w}_i = 0$$

(4.17) & (4.18)

Once the last point of the prediction is located, the potential energy peak method along a ray starting at the s.e.p. and the last point of the prediction is computed. However, the ray method might not sense any potential energy peak. Therefore, the Ball-Drop method has been set up. In this method, an operating point is found to be inside or outside the p.e.b.s. by a single, path independent procedure. Starting with a zero velocity, the method integrates a trajectory in the reduced system given by equation (5.1). At the end of the integration, the location of the new state is compared to the old one by their respective distances from the post-fault s.e.p. If the distance is increasing, the system is assessed to be beyond the p.e.b.s. Finding a good step size for the integration is critical. To determine the impact of the step size on the integration, several simulations were repeated using different step sizes. By increasing it from 0.005 to 0.05 second, we found that there is no significant loss in the accuracy. However, the gain in computation time is significant. It can be reduced by a factor of ten. Further increase in the step size from 0.05 second to 0.1 second causes appreciable error in the energy calculation. To bring further improvement in the computation speed, a trapezoidal method to integrate the gradient system could allow a time step larger than 0.05 sec.